THE EFFECTS OF WALL ROUGHNESS ON THE TURBULENT BOUNDARY LAYER

L. Vesely*, C. Haigermoser*, M. Onorato*
***Politecnoco di Torino**
Dipartimento di Ingegneria Aeronautica e Spaziale

Keywords: *boundary layer, turbulence, roughness*

Abstract

The Turbulent flows over a zero-pressure-gradient boundary layer are investigated to observe the effect of a 2-dimensional wall wavy roughness, perpendicular to the mean flow, and of two 3-dimensional wall roughness on the organization of the coherent motions characterizing the turbulent flow. Particle image velocimetry is used to describe instant flow fields in the streamwise plane normal to the wall and in planes parallel to the wall. In the outer layer the organization of coherent motions appears to be very similar to the one observed for the case of a smooth wall. Two-point spatial correlations of the longitudinal and wall normal velocity fluctuations suggest the recurrence of packets of hairpin vortices travelling coherently as expected in a turbulent boundary layer over a smooth wall. The flow velocity correlations enlighten differences in scale and orientation of the structures.

1 Introduction

The investigation of turbulent boundary layers on rough walls remains an important subject for engineering applications, but also for fundamental research. The prediction of the effect of wall roughness on boundary layers is an important subject for applications to ship hulls and airplanes, for the transport of fluids in ducts and for the heat transfer in heat exchangers. This has been the main reason for promoting a large body of research on wall-bounded shear flows with roughness. Reviews of much of this work are given by [13] and [17]. Moreover the study of rough wall boundary layers is also an interesting subject to try to give a contribution to a better understanding of the dynamics of wall turbulence.

It is well known that most of the observed phenomena characterizing the turbulence effects on near wall flows, as the increase of skin friction and heat transfer, the high level of velocity fluctuation, the bursting events and the organization of the near wall flow in high and low speed streaks, are due to the random presence of organized motions (coherent structures), consisting in trains of streamwise elongated vortical structures ([1]; [9], [12], [18]).

In an attempt to give a contribution to the understanding of the effects of wall roughness on the dynamics of the turbulent organized motions, Particle Image Velocimetry experiments are conducted at the Politecnico di Torino Aerodynamic Laboratory on zero pressure gradient rough walls. Results are shown in the present paper for a wall roughened by 2D grooves perpendicular to the mean flow and for two 3D surfaces roughened by pyramids with different orientation to the mean flow. The results are compared with smooth wall data.

2. Experimental set up

The experiments were carried out in the water tunnel at the “Dipartimento di Ingegneria Aeronautica e Spaziale” of the Politecnico di Torino. This facility is a closed-loop open-surface channel with a 350x500x1800 mm^3 test section. The external free-stream turbulence level was 2% and the maximum ratio for the boundary layer thickness to the width of the tunnel was 0.15, ensuring that the mean boundary layer on the flat plate was two dimensional over the central 70% of its width.

Measurements were taken on a flat plate with a length of 2050 mm (Fig.1). Two-dimensional roughness, consisting of grooves perpendicular to the flow and of two different geometries of three-dimensional roughness, were glued over the surface of the flat plate (Fig.2). The two 3-D roughness consisted respectively by pyramids aligned with the flow and by pyramids inclined 45° with respect to the flow, as shown in Fig.2. The roughness material was black rubber. At the flat plate leading edge the laminar-turbulent transition was imposed by a sand paper.
Measurements were taken with a time resolved PIV System, which consisted of a 1280x1024 pixels high speed NanoSense MKIII CMOS camera and a continuous Spectra-Physics Argon laser, with a maximum emitted power of 6W. The maximum acquisition rate of the camera, at full resolution, was 1024 Hz, which allowed to perform time-resolved measurements. The laser beam was expanded by a cylindrical lens and focused by a spherical lens, forming a light sheet with a thickness of about 0.5 mm. The PIV system consisted further of "DANTEC Flow Manager" software to perform the correlations to obtain the velocity fields. The water was seeded with spherical Silicon Carbide particles, 2 μm nominal diameter, which were small enough to follow the flow faithfully. The particle density was approximately 0.05 particles per pixel. PIV measurements were taken in the streamwise wall-normal plane (x,y) and in the plane parallel to the wall (x,z), 1750 mm downstream from the flat plate's leading edge. The physical size of the PIV images in the plane (x,y) ranged from 52x42mm^2 (690x560 viscous units) for the smooth wall to 68x54mm^2 (1370x1080 viscous units) for 3D-45°. In all the cases, the PIV images covered the whole boundary layer thickness. In the planes parallel to the wall the physical size for all walls was about 51x41mm^2, which corresponds to size in viscous units from (680x550 viscous units) to (1020x820 viscous units), respectively for the smooth and the 3D-45° walls. The local particle displacements were determined using an adaptive cross correlation algorithm. The final interrogation window size was 32x32 pixels, overlap of 50%. The obtained vectors were validated using a minimum peak height in the correlation, which was 1.2 times the height of the second highest peak. Erroneous vectors were substituted by vectors found by a moving average filter using the surrounding vectors with neighbourhood size of 5x5 vectors.

3 Experimental conditions and mean velocities

The experimental test conditions are given in Table 1. The value of the Reynolds numbers, based on the boundary layer momentum thickness, θ, ranges from 930 for the smooth wall to 2060 for the 3D-45° rough surface. This characterizes the present results in the range of relatively low Reynolds numbers. The difference in Re_θ between the different cases is due to the boundary layer thickness, that is significantly higher for the flow over the rough surfaces. The friction velocity U_τ, obtained by the modified Clauser chart method ([16]), as expected, increases largely for the case of rough walls. The boundary layer thicknesses and the equivalent sand grain roughness height, k_s, also increase for the rough surface case.

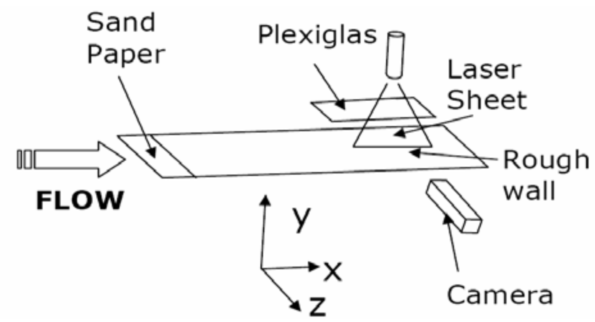

Fig.1 Experimental set-up for measurements in the plane (x,y).

[3] found that the effect of roughness on the mean flow was confined to the inner layer, causing only a downward shift in the smooth wall log-law ΔU^+. They extended the log-law to the case of rough wall boundary layers as

$$U^+ = 1/k \ln(y^+) + B - \Delta U^+$$

where U is the mean velocity, k = 0.421 is the Karman constant, y is the distance from the virtual origin, B = 5.2 is the smooth wall log-law intercept and ΔU^+ is the roughness function. The virtual origin is evaluated according to [16]. The apex plus indicates that the quantity has been normalized with respect to the wall units. The measured values of ΔU^+, reported in Table 1, show that, according to [10], the 3D-45° roughness affects more deeply the near wall flow than the 3D-0° and 2D roughness.

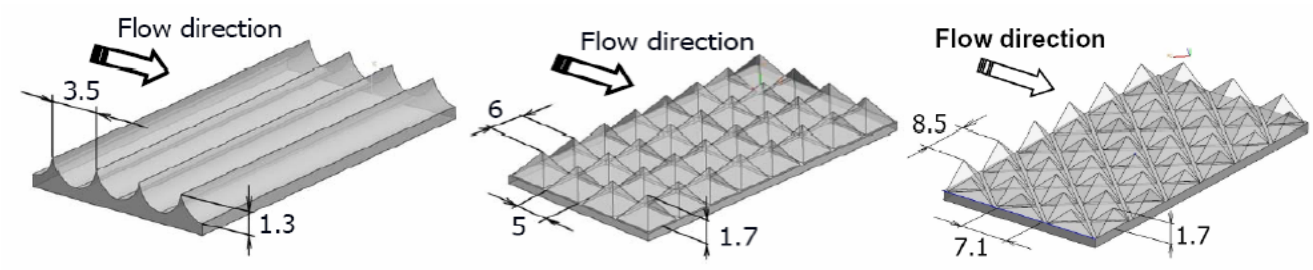

Fig.2 Roughness geometries. Dimensions in mm.

Table 1

Wall surface	K [mm]	U_e [m/s]	θ [mm]	δ [mm]	δ* [mm]	Re_θ [-]	H [-]	U_τ [m/s]	k_S [mm]	k_S^+ [-]	δ/k [-]	δ/k_S [-]	ΔU^+ [-]
Smooth	**-**	**0.29**	**3.3**	**32.7**	**4.9**	**930**	**1.5**	**0.0138**	**-**	**-**	**-**	**-**	**-**
2D	**1.3**	**0.29**	**4.8**	**37.3**	**7.4**	**1360**	**1.5**	**0.0195**	**4.71**	**90.2**	**28.6**	**79**	**7.7**
3D-0°	**1.7**	**0.29**	**5.3**	**39.6**	**8.1**	**1515**	**1.5**	**0.0197**	**9.82**	**198**	**23.3**	**40**	**9.6**
3D-45°	**1.7**	**0.29**	**7.3**	**51.3**	**11.8**	**2060**	**1.6**	**0.0200**	**13.7**	**273**	**30.2**	**37**	**10**

Mean velocity profiles plotted in inner variables are shown in Fig.3 for the four flows. The smooth wall LDV measurements of [5] at Re_θ = 1430 compares satisfactory well with the present results, except in the first point very close to the wall. The three rough surfaces display a linear log region shifted below the smooth profile of a quantity corresponding to the roughness function, ΔU^+. Despite the relatively low Reynolds numbers, the log regions are clearly identified. The values of ΔU^+ are reported in Table1.
Fig.4 presents the mean velocity profiles in velocity defect form, using classic inner-outer scaling by U_τ and δ, for the smooth and the 2D rough walls. To establish if the outer layer similarity hypothesis holds, the error bands are indicated in correspondence of the measurements points. Error bands relative to y/δ, evaluated as ±4%, are omitted. The evident collapse of the two velocity profiles for smooth and 2D rough walls, behind y/δ = 0.05, even inside the roughness layer height evaluated at y/δ = 0.2, indicates that, for the present 2D roughness geometry, the mean flow is largely insensitive to the surface conditions.

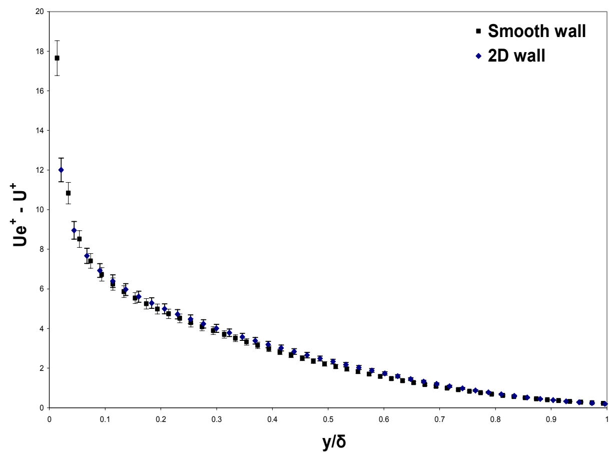

Fig.4 Mean velocity profiles in velocity defect form. Error bars: 5%.

Conversely to the case of the 2D wall roughness, the flow over the two pyramidal rough walls does not appear to show outer layer similarity, as demonstrated in Figs.5 and 6. The mean velocity profiles in velocity defect form are far from collapsing,

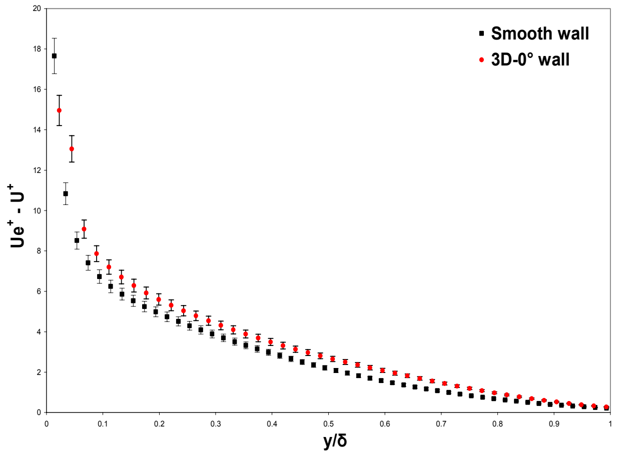

Fig.5 Mean velocity profiles in velocity defect form. Error bars: 5%.

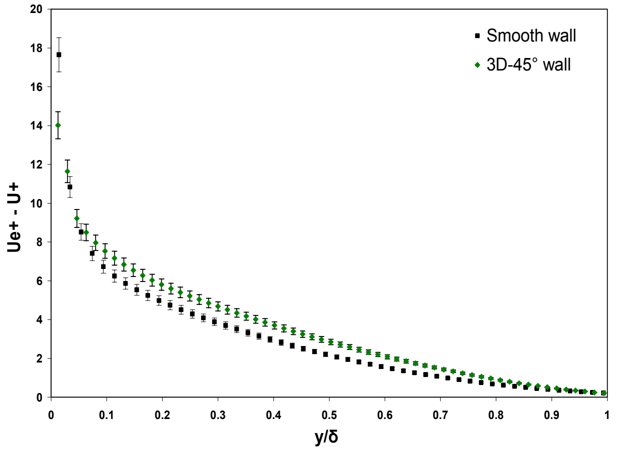

Fig.6 Mean velocity profiles in velocity defect form. Error bars: 5%.

The inconsistency between the present results for the two 3D rough walls and the results in [7], where outer layer similarity was found behind the roughness layer, for roughness heights even larger than the ones in the present paper ($\delta/k = 21, 19, 16$ or $\delta/k_s = 11, 7, 5.5$), may be explained with reference to Reynolds number effects. According to [13], both the roughness height and the viscous scale must be small compared to the outer flow scale (δ) to expect outer layer similarity conditions. This is not the case of the present relatively low Reynolds number data.

Mean velocities expressed in defect low for the two 3-D wall roughness (not shown here) collapse, except in the very near wall region ($y/\delta < 0.1$), even if they show substantial differences in skin friction, roughness function and boundary layer thickness.

4 Turbulence structure in planes (x,y)

No obvious imprint of the wall roughness on the flow in the outer region is evident observing single instant PIV images. Statistical analysis may enlighten possibly existing quantitative differences between the two flow fields over smooth and rough walls.

In Figs.7 and 8 contours of constant values of the two point streamline and wall normal velocity auto-correlation functions, $\rho_{u'u'}$ and $\rho_{v'v'}$, at $(y/\delta)_{ref} = 0.5$, are respectively displayed, for the cases of the smooth and rough walls normalized with respect to the boundary layer thickness. The shape of the contours $\rho_{u'u'} = const.$ for the three rough walls are similar to the ones for the case of the smooth wall (Fig.7a) and to the one found (among others) by [14] in a channel flow. They appear elongated in the mean flow direction and inclined at a shallow angle to the wall. A different behaviour of the wall normal velocity correlation function, $\rho_{v'v'}$, is observed in Figs.8, for the smooth and rough walls. The v'-correlation appears to have roughly circular contours, in evident contrast to the elongated shapes of the u'-component correlation. $\rho_{v'v'}$ contours are compact in both streamwise and wall normal directions and show an extent relatively small with respect to the u'-correlation in the mean flow direction.

The characteristic shape of the streamwise and wall normal velocity correlations in Figs 7 and 8, reflects the organization of the near wall eddies into packets travelling coherently with uniform velocity. This is consistent with the conjecture that the flow is dominated by a series of hairpin vortices aligned in the streamwise direction, whose heads lie along a line inclined away from the wall, as claimed by [4], for a smooth wall.

The inclination angle of the contours $\rho_{u'u'}$ defines the orientation of these dominant flow structures. Within an individual eddy the streamwise and wall normal scales are expected to be similar, but the assembly of the eddies in a coherent packet has much longer scale. The long u'-correlation is associated with the coherent induction of many vortical structures in the packet; while the short v′-correlation is associated with the scale of individual eddies ([14]).

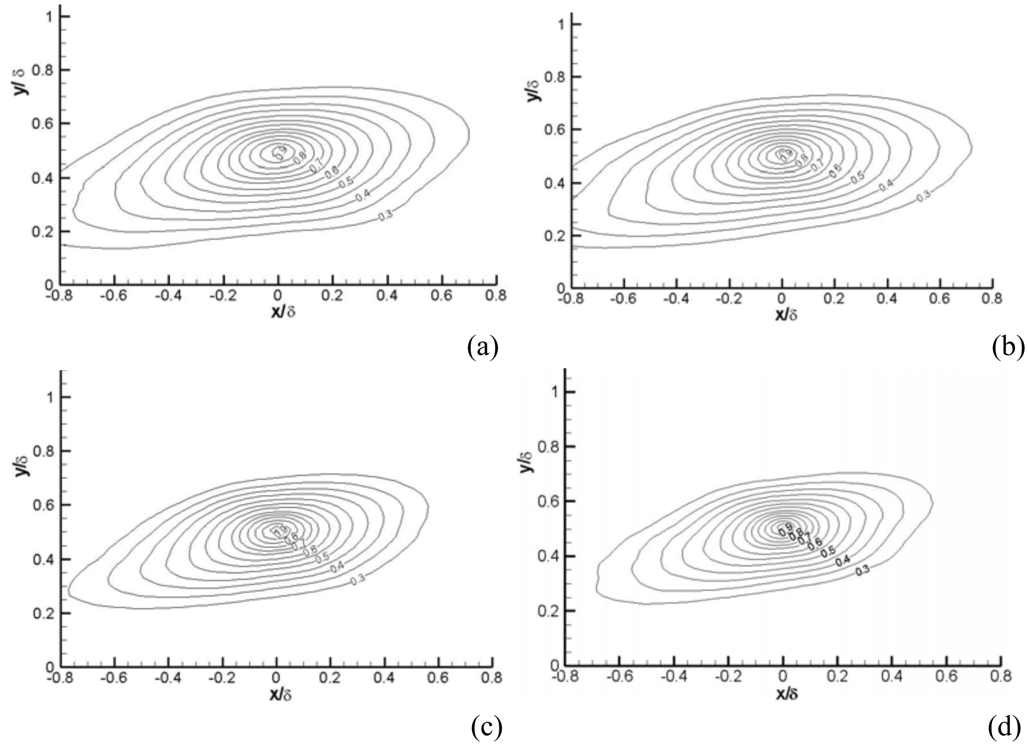

Fig. 7 Contours of constant values of the two point streamwise velocity auto-correlation function. $(y/\delta)_{ref.} = 0.5$. (a): smooth wall; (b): 2D wall; (c): 3D-0° wall; (d): 3D-45° wall.

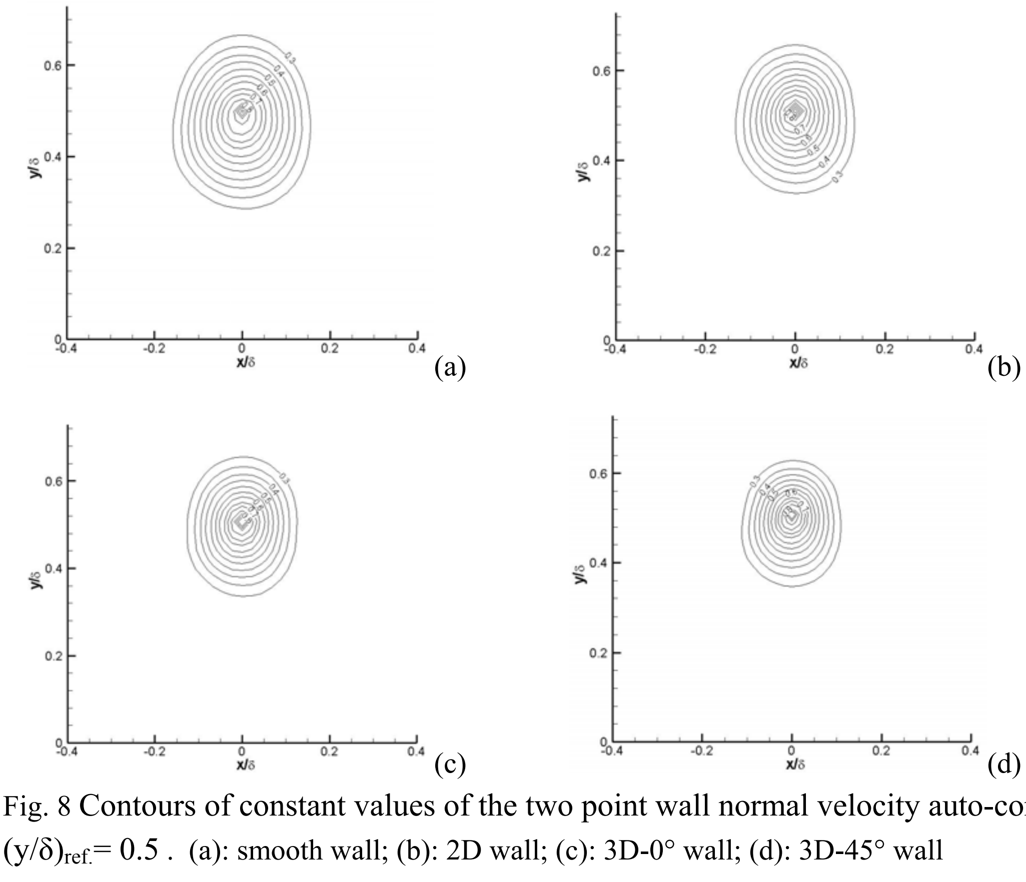

Fig. 8 Contours of constant values of the two point wall normal velocity auto-correlation function. $(y/\delta)_{ref.} = 0.5$. (a): smooth wall; (b): 2D wall; (c): 3D-0° wall; (d): 3D-45° wall

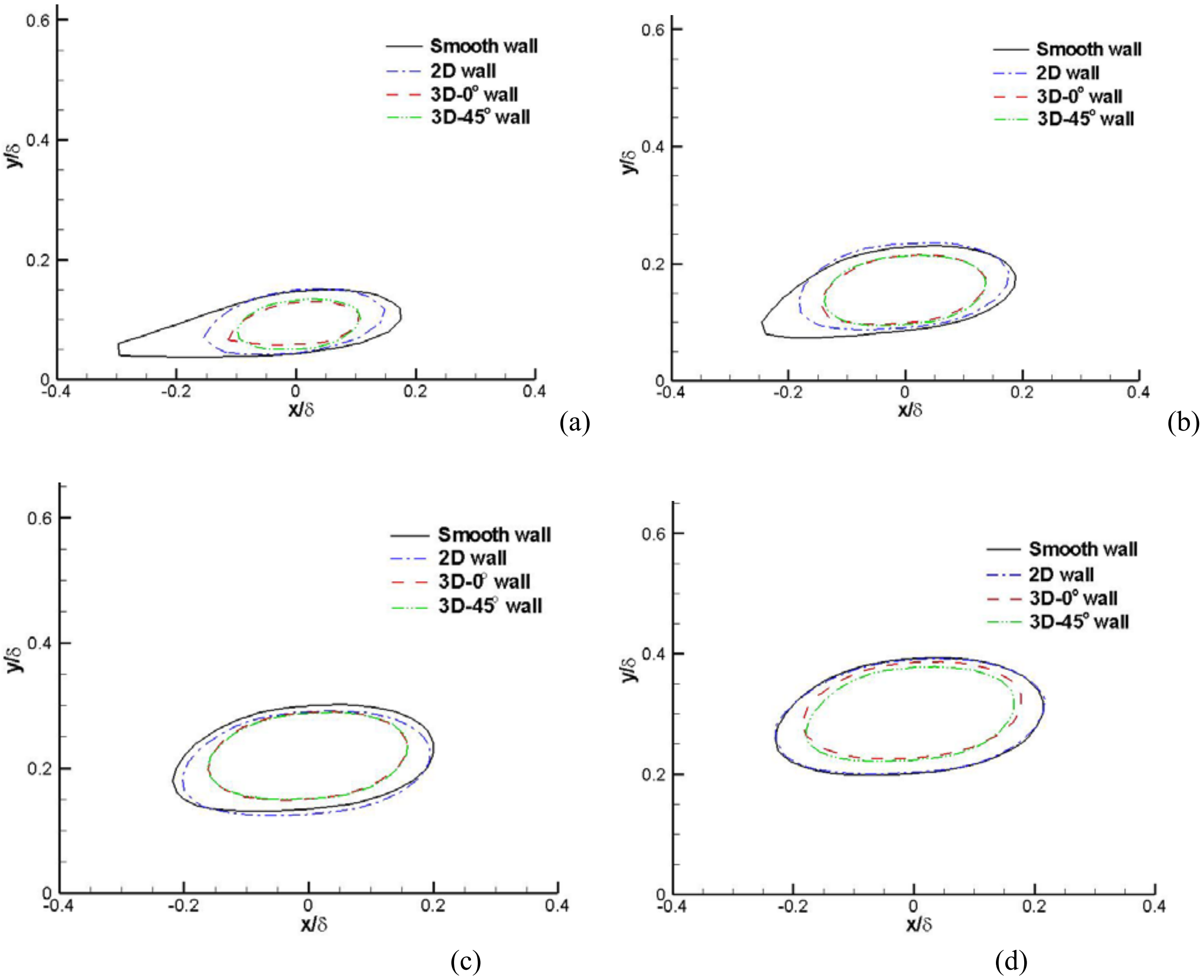

Fig. 9 Contours of constant values of the two point streamwise velocity auto-correlation function, $\rho_{u'u'}$ = 0.6. (a): $(y/\delta)_{ref.}$= 0.1: (b): $(y/\delta)_{ref.}$= 0.15; (c): $(y/\delta)_{ref.}$= 0.2; (c): $(y/\delta)_{ref.}$= 0.3.

The inclination of the contours $\rho_{u'u'}$= const. in Figs.7 and in Figs.9 for the four walls, ranges from 9° to 14°, depending on the distance from the wall of the correlation reference point. [14] found for smooth wall, in a channel flow, an inclination angle of 6-8 degrees. An average angle of about 10 degree is also reported in [11] for smooth wall. A different result was reported in the same paper for a wall roughened by a screen corresponding to a sand roughness of $k_s^+ = 331$, calculating correlations from time velocity series measured using a rake of x-wires. They found a very large inclination angle of 38°. They attributed the increase of this angle to the reduced damping of the wall-normal velocity fluctuations close to the rough surface and to the break-up of small structures whose scale are comparable to the size of roughness elements. [11] results are not corroborated by similar experimental results by other authors. [15], analyzing PIV results in a channel flow over a two-dimensional sinusoidal roughness $(\delta / k \approx 60)$, producing a roughness function ΔU^+=8.12, measured a slope angle of 9°, very close to the one measured in the present experiment.

Observing results from quadrant analysis of a flow over two three-dimensional rough surfaces, sandpaper and woven mesh, [7] show that roughness induced changes to the coherent turbulent structures are confined to a near-wall roughness sublayer, extending 3k-5k from the wall. In their paper the ratio δ / k ranges from 45 for the sandaper ($\delta / k_s = 62$) to 100 for the mesh ($\delta / k_s = 45$). [20], testing surfaces containing a broad range of topological scales produced by deposition of foreign materials on the surface ($\delta / k = 25 - 28$ and $\delta / k_s > 40$), measured two point spatial velocity correlation coefficients obtaining results sensitive to the surface topology, as smooth and rough data showed measurable differences.

Back to Figs.9, they show interesting features both in the roughness layer (y/δ < 0.2) and in the outer layer. Far from the wall (Figs.9 c,d,e) the contours $\rho_{u'u'}$ = 0.6 for the smooth and 2D walls are very close (indistinguishable at $(y/\delta)_{ref}$ = 0.2), suggesting similar longitudinal and wall normal scales, when lengths are normalized with respect to the boundary layer thickness. Also the correlation contours of the two 3D rough walls collapse between them, but showing a moderately smaller extent in the x/δ and y/δ directions with respect to the smooth wall.

The effect of the wall roughness is evident very near the wall (Figs.9a and b), where the longitudinal length-scale for the flow over the smooth surface appears much larger than the one over the roughened surfaces. This confirms the observation of [2]. They also found that the turbulence integral length scale in the streamwise direction was shorter for the case of rough surfaces with respect to the case of a smooth wall, indicating a break-up of the near-wall streamwise vortices over the rough wall.

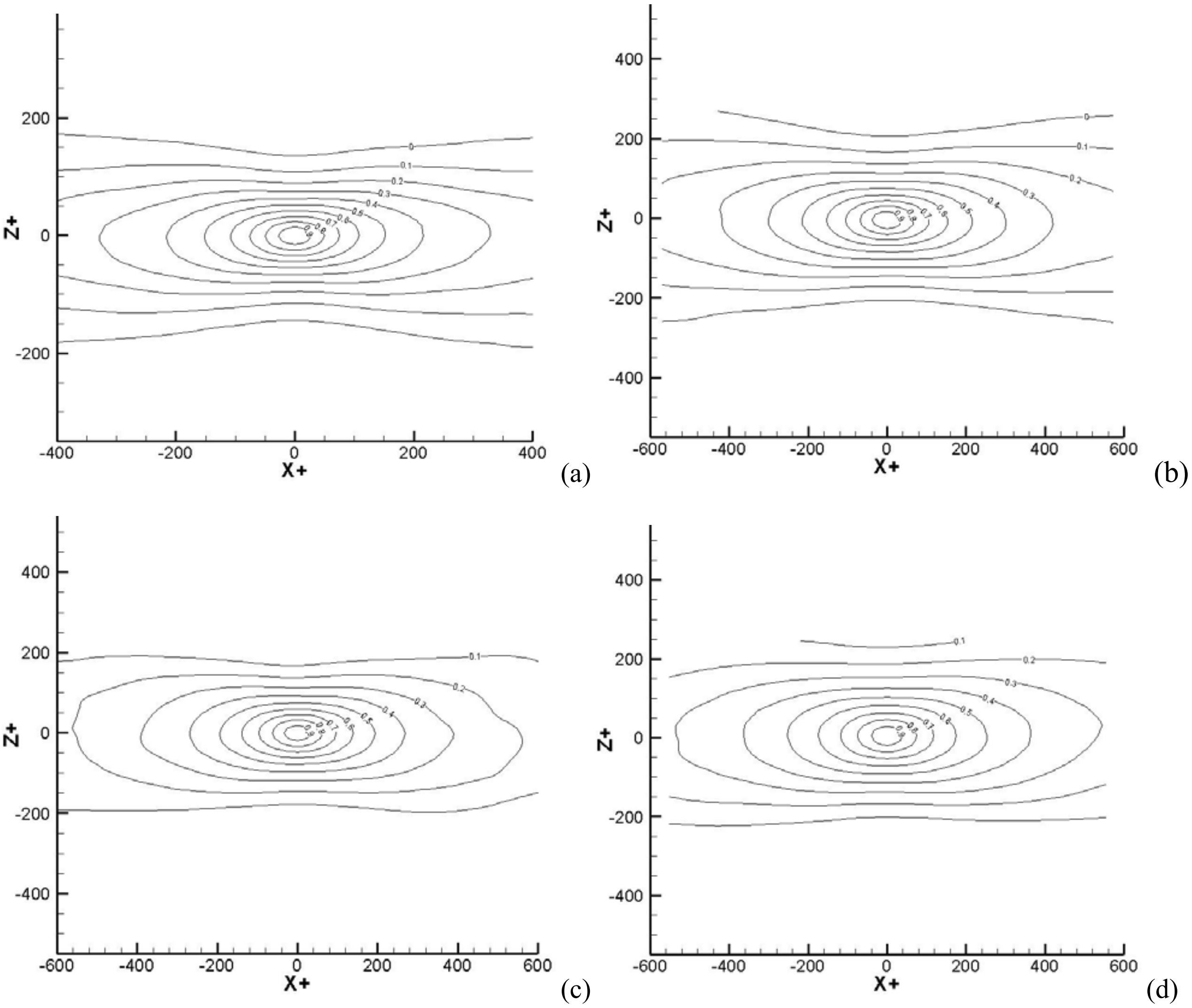

Fig.10 Two point streamwise velocity auto-correlation function in the plane y/δ = 0.3. (a): smooth wall, (b): 2Dwall, (c): 3D-0° wall, (d): 3D-45° wall.

5 Turbulence structure in plane (x,z)

In Figs.10 contours of constant values of the two point streamwise velocity auto-correlation function, in the planes y/δ = 0.3 are displayed for the cases of the smooth and rough walls. Clearly visible is the characteristic elliptical shape of the correlation, with the principal axis elongated in the streamwise direction, for both the smooth and the rough walls. The long streamwise coherence could be caused either by long zones of negative u' induced by the packets of vortical structures or by zones of positive u', sometimes present on either side of the packets ([8]). The flow structure for the different walls, at y/δ = 0.3, as well as in other planes in the outer layer, appears similar.
In order to examine the influence of the wall roughness geometries on the scales of such large scale structures, direct comparisons between $\rho_{u'u'}$ correlations for the different flows are shown in Fig.11. The extent of the regions where $\rho_{u'u'}$ is equal 0.6 has been chosen to be representative of the topology and the dimension of the structures. The comparisons shown in Figs.11 (a) and (b), respectively for y/δ = 0.2 and y/δ = 0.3, confirms what has been found in the streamwise-wall-normal plane. The correlation functions show satisfactory collapse between the smooth and the 2D walls and between the two 3D walls, when quantities are normalized with respect to the boundary layer thickness. Moreover, the length and width of the correlation are both larger for the smooth and the 2D walls with respect to the ones for the 3D roughness, showing higher streamwise and spanwise scales in the former case.

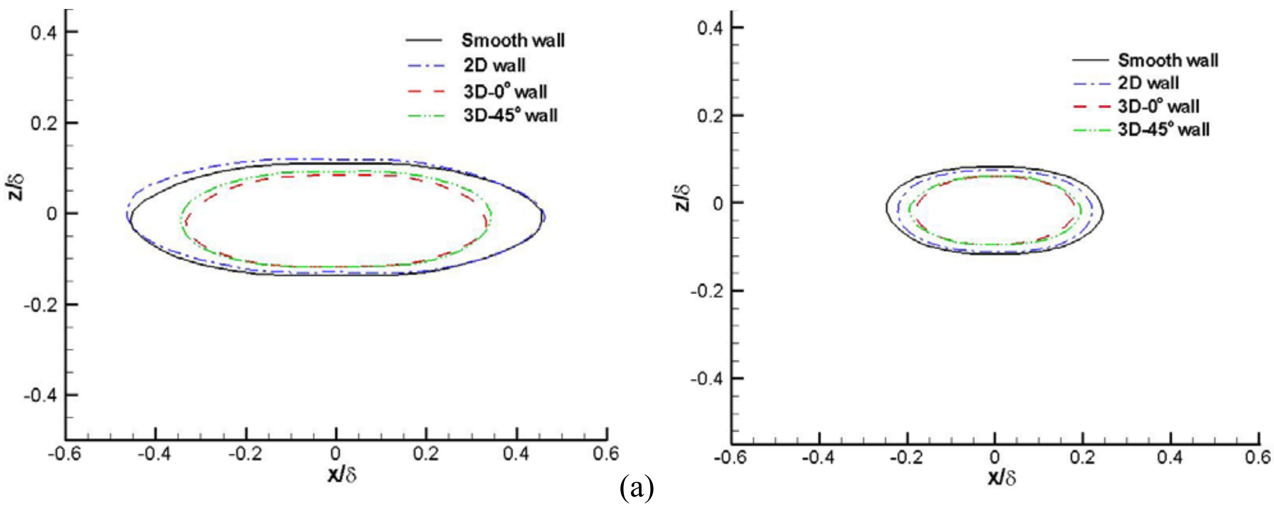

Fig.11 Two point streamwise velocity auto-correlation function $\rho_{u'u'}$ = 0.6 in the planes y/δ = 0.2 (a) and y/δ = 0.3 (b).

Similar flow organization may also be seen in the roughness layer, near the wall, but above the roughness, in Fig.12, where lengths are now normalized with respect to inner variables. The shape and the width of the correlation function in the buffer layer in the case of the smooth wall, correspond quantitatively to what is expected in a canonical turbulent boundary layer, showing a streamwise extension of more than 1000 viscous length and a spanwise extension of about one hundred viscous lengths. The last corresponds to the well assessed mean spacing between the low speed streaks, in the lower part of the buffer layer. The corresponding correlation for the rough walls shows a wider spanwise extension and nearly the same streamwise length, when normalized with inner variables.

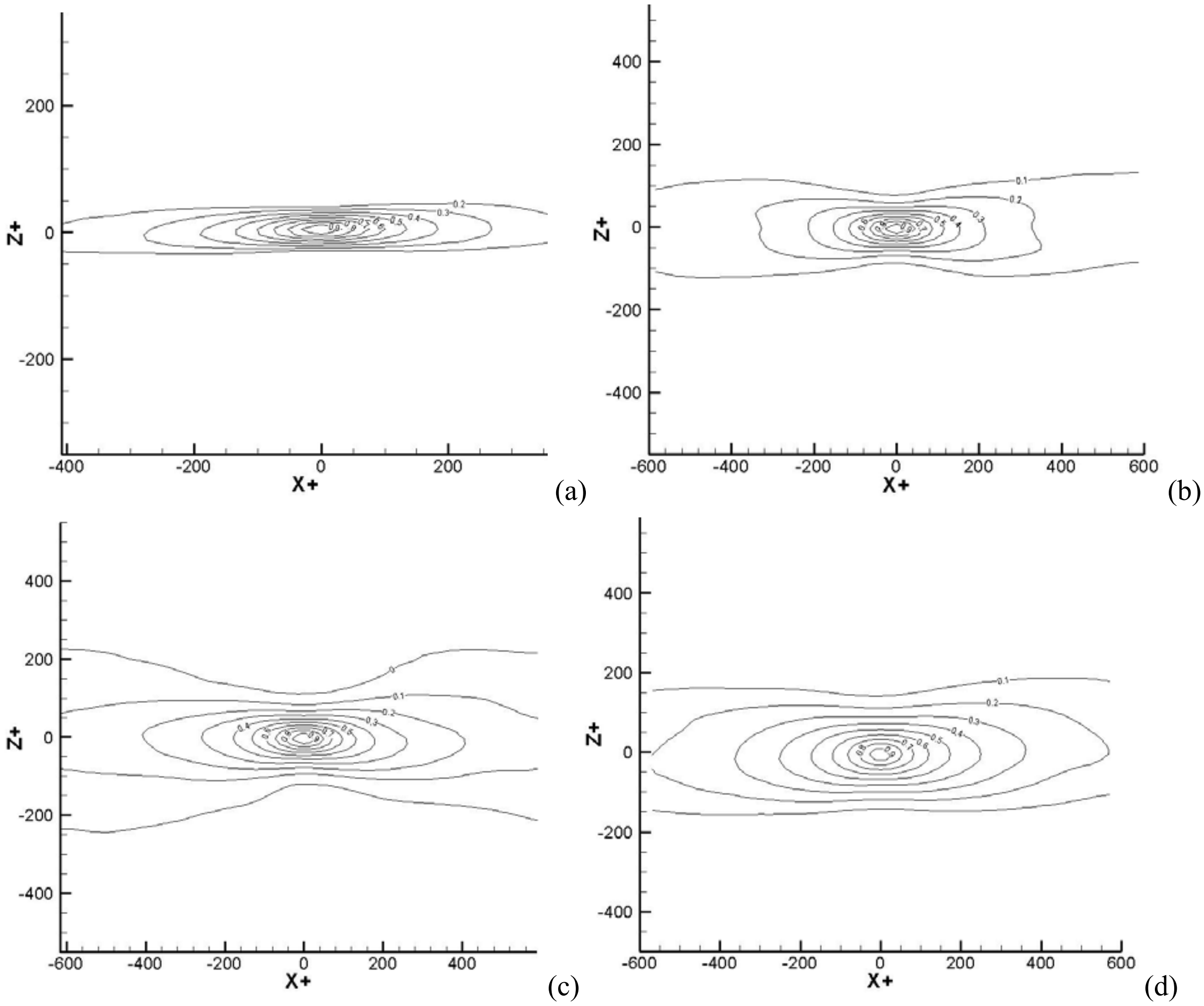

Fig.12 Two point streamwise velocity auto-correlation function in the plane $y/\delta < 0.1$. (a): smooth wall, (b): 2D wall, (c): 3D-0° wall, (d): 3D-45° wall.

6.Conclusions

PIV measurements at relatively low Reynolds numbers in turbulent boundary layers over 2D and 3D roughened surfaces have been presented and compared to those for a smooth wall. Mean flow expressed in velocity defect law shows excellent agreement in the outer layer between the 2D roughened wall and the smooth wall, providing support for the wall similarity hypothesis ([17]; [19]). This result occurs in spite of the relatively high value of the roughness thickness ($\delta/k \approx 29$; $\delta/k_s \approx 80$) and the relatively low Reynolds numbers, $Re_\theta = 930$ and 1360, respectively for the smooth and rough wall. Conversely outer layer similarity is not observed between the flow over the two 3D roughened surfaces and the smooth wall, showing in this case that the outer layer was not independent of the surface condition. This result apparently contrasts with the recent study of [7], where roughness influence in the outer layer was not observed for $\delta/k \geq 19$ or $\delta/k_s \geq 5.5$ and it was not observed a critical roughness height that produces modifications to the outer layer turbulence statistics. It is opinion of the present authors that the observed differences must be attributed to the much lower Reynolds number of the present experiments, but also to the different geometries of the tested roughness.

Mean velocity expressed in defect low, except in the very near wall region ($y/\delta < 0.1$), collapses for the two 3-D wall roughness, even if they show substantial differences in skin friction, roughness function and boundary layer thickness.

Two point streamwise velocity auto-correlation functions, in the outer layer, in the plane (x,y), suggest that packets of vortical structures are coherently aligned with an inclination angle (with respect to the wall) ranging from 9 to 14 degree, depending on the distance from the wall and very close to the inclination found in the present study and the one reported in several papers for the case of the flow over a smooth surface. The packet's overall scales (here evaluated as fraction of the boundary layer thickness) appear slightly larger for the smooth and the 2D case with respect to the two 3D roughness cases. This is confirmed by the auto-correlation function contours in planes (x,z), for $y/\delta \geq 0.2$, where the correlation function contours for the smooth and the 2D walls are about indistinguishable between them and slightly larger than the ones for the two 3D surface cases, showing slightly larger streamwise and spanwise scales. The correlation functions for the flows over the two 3D surfaces are also roughly indistinguishable between them.
Different situation is observable very near the wall, $y/\delta < 0.1$, in both the (x,y) and (x,z) planes, where the correlation functions for the case of the smooth wall shows a much larger streamwise scale with respect to the rough wall cases, including the 2D wall case (see Figs.9 and 12). This clearly indicates a loss of longitudinal coherence due to the action of the surface roughness. Also the spanwise scale shows a different character in the case of rough surfaces with respect to the smooth wall. It appears much larger, assuming values much higher than the expected typical values from about 100 to 200 wall units in the buffer layer of a canonical turbulent boundary layer. All this indicates that the expected organization in the buffer layer of the flow in longitudinal coherent high and low speed streaks is strongly influenced by the wall roughness.

References

[1] Adrian R.J., Meinhart C.D., Tomkins C.D. *Vortex organization in the outer region of the turbulent boundary layer*. J. Fluid Mechanics 422, pp.1-54, 2000.

[2] Bakken O.M., Krogstad P.A., Ashrafian A., Andersson H.I. *Reynolds number effects in the outer layer of the turbulent flow in a channel with rough walls*. Phys. Fluids 17, article 065101, 2005.

[3] Clauser F.H. *Turbulent boundary layers in adverse pressure gradient*. J. Aeronaut. Sci. 21, 91, 1954.

[4] Christensen K.T., Adrian R. J. *Statistical evidence of hairpin vortex packets in wall turbulence*. J. Fluid Mech. 431, pp.433-443, 2001.

[5] De Graff D.B., Eaton J.K. *Reynolds-number scaling of the flat-plate turbulent boundary layer*. J. Fluid Mech. 422, pp.319-346, 2000.

[6] Flack K.A., Schultz M.P., Connelly J.S. *Examination of a critical roughness height for outer layer similarity*. Phis. Fluids 19, pp. 095104, 2007.

[7] Flack K.A., Schultz M.P., Shapiro T.A. *Experimental support for Townsend's Reynolds number similarity hypothesis on rough wall*. Phys. Fluids 17, article 035102, 2005.

[8] Ganapathisubramani B. Longmire E.K., Marusic I. *Characteristics of vortex packets in turbulent boundary layers*. J. Fluid Mech. 478, pp. 35-46, 2003.

[9] Gottero M., Onorato M. *Low speed streak and internal shear layer motions in a turbulent boundary layer*. Eur. J. Mech. B-Fluids 19, pp23-36, 2000.

[10] Hama F.R. *Boundary layer characteristics for rough and smooth surfaces*. Trans. SNAME 62, pp. 333-351, 1954.

[11] Krogstad P.A., Antonia R.A. *Structure of turbulent boundary layers on smooth and rough walls*. J. Fluid. Mech. 277, pp. 1-21, 1994.

[12] Jeong J., Hussain F., Schoppa W., Kim J. *Coherent structures near the wall in a turbulent channel flow*. J. Fluid Mech. 332, pp. 185-214, 1997.

[13] Jimenez J. *Turbulent flow over rough walls*. Annu. Rev. Fluid Mech. 36, pp. 173-196, 2004.

[14] Liu Z., Adrian R.J., Hanratty T.J. *Large-scale modes of turbulent channel flow: transport and structure*. J. Fluid Mech. 448, pp. 53-80, 2001.

[15] Nakagawa S., Hanratty T.J. *Particle image velocimetry measurements of flow over a wavy wall*. Phys. Fluids 13, N.11, pp. 3504-3507, 2001.

[16] Perry A.E., Li J.D. *Experimental Support for the attached-eddy hypothesis in zero-pressure gradient turbulent boundary layers*. J. Fluid Mech. 218, pp. 405-438, 1990.

[17] Raupach M.R., Antonia R.A., Rajagopalan S. *Rough-wall turbulent boundary layers*. Appl. Mech. Rev. 44, pp. 1-25, 1991.

[18] Robinson S.K. *Coherent motions in the turbulent boundary layer*. Annu. Rev. Fluid Mech. 23, pp. 601-639, 1991.

[19] Townsendt A.A. *The structure of turbulent shear flow* 2nd edn. Cambridge University Press, 1976.

[20] Wu Y., Christensen K.T. *Reynolds-stress enhancement associated with a short fetch of*

roughness ib wall turbulence. TAM Report 1085, University of Illinois, Urbana, 2006.

Copyright Statement